Radiology

TIPS for Better Browsing

Institution: NYU Medical Center || Sign In as Member || Contact Subscription Administrator at this Site || **FAQ**

- Abstract of this Article
- Figures Only for this Article
- **Reprint (PDF) Version of this Article**
- eLetters: **Submit a response** to this article
- Similar articles found in:
  Radiology Online
- Search Medline for articles by:
  Ko, J. P. || Betke, M.
- Alert me when:
  new articles cite this article

Technical Developments

Chest CT: Automated Nodule Detection and Assessment of Change over Time—Preliminary Experience[1]

Jane P. Ko, MD and Margrit Betke, PhD

[1] From the Department of Radiology, Massachusetts General Hospital, Boston (J.P.K.); and the Computer Science Department, Boston University, Boston, Mass (M.B.). Received January 20, 2000; revision requested March 3; revision received April 25; accepted May 1. **Address correspondence to** J.P.K., Department of Radiology, New York University Medical Center, 560 First Ave, New York, NY 10016 (e-mail: *jane.ko@med.nyu.edu*).

ABSTRACT

- Top
- ABSTRACT
- INTRODUCTION
- Materials and Methods
- Results
- Discussion
- REFERENCES

The authors developed a computer system that automatically identifies nodules at chest computed tomography, quantifies their diameter, and assesses for change in size at follow-up. The automated nodule detection system identified 318 (86%) of 370 nodules in 16 studies (eight initial and eight follow-up studies) obtained in eight oncology patients with known nodules. Assessment of change in nodule size by the computer matched that by the thoracic radiologist (Spearman rank correlation coefficient, 0.932).

Index terms: Computed tomography (CT), computer programs • Computed tomography (CT), image processing • Computers, diagnostic aid • Lung, nodule, 60.281

▶ INTRODUCTION

In the United States, about 8 million people have a history of cancer, either cured or in the process of being treated, and predictions indicated that 1.2 million new diagnoses of invasive cancer would be made in 1999 (1). Extrathoracic and thoracic malignancies frequently metastasize to the lung parenchyma as pulmonary nodules, and the most sensitive diagnostic imaging modality for detecting such nodules is computed tomography (CT) of the thorax. To assess disease progression or regression with therapy when metastatic disease to the lung is discovered, precise quantitative and reproducible analysis is required of what is often a large number of nodules. Computer schemes are therefore needed that help (*a*) improve nodule detection by the radiologist, (*b*) quantify nodule volume and number, and (*c*) assess change in nodule number and diameter.

To our knowledge, research about automated assessment of change in nodule number and size has not been performed previously. Studies have primarily addressed automated nodule detection at CT (2–5) and chest radiography (6,7). Findings demonstrate that computer-aided diagnosis systems help improve a radiologist's receiver operating characteristic curve for detecting pulmonary nodules (8) and characterizing interstitial lung disease (9) on chest radiographs. However, there is a need to better quantify the size of pulmonary nodules and their change over time. To estimate change in nodule volume, the radiologist typically uses bidimensional measurements in the transverse plane. These measurements are subject to inter- and intraobserver variations, which can be decreased with a computer system. Yankelevitz et al (10) demonstrate that growth in malignant tumors as small as 5 mm can be detected at early repeat CT with use of a semiautomated method.

A computer system for automated nodule detection and quantification capabilities could be applied to a high-volume screening scenario such as low-dose CT, which has been studied as a screening test for lung cancer in a high-risk population (11). The failure to identify a nodule at low-dose CT (12) may crucially affect a patient's prognosis, and a vision system could help decrease the number of missed nodules.

Given the potential applications to treatment and screening of patients with cancer, we developed a computer vision system that not only detects pulmonary nodules at CT but also quantifies their volume and change over time. The purpose of this study was to evaluate the performance of the computer vision system.

▶ Materials and Methods

Patient Data

Eight patients with cancer diagnoses and pulmonary nodules were selected from the patients who

underwent thoracic CT at Massachusetts General Hospital (Boston) for clinical indications from January 1998 through August 1999. To select patients, we used a computer program (FOLIOVIEWS, version 3.1; InfoArchiText, Newton, Mass) that searched radiology reports of chest CT scans for the terms "pulmonary nodules" and "cancer." Patient reports were selected at random from search results. A patient was excluded if the reports included the terms "lung cancer," "consolidation," or "collapse," or if the patient did not undergo follow-up CT at our institution. This process was repeated until eight patients with 16 studies (eight initial and eight follow-up studies) were selected. The cases of the patients were labeled with a letter A through H followed by either a 1 or 2 to represent the initial or follow-up CT study, respectively. The time interval between the two CT studies was 5 ($n = 1$), 2.5 ($n = 1$), 2.25 ($n = 2$), 2 ($n = 1$), and 1.5 ($n = 3$) months. Each patient's clinical course and diagnosis was confirmed by means of chart review. Patient diagnoses were renal ($n = 1$), esophageal ($n = 1$), neuroendocrine ($n = 1$), colorectal ($n = 2$), and bladder ($n = 1$) carcinomas, as well as melanoma ($n = 1$) and sarcoma ($n = 1$).

The chest helical CT studies (HiSpeed Advantage; GE Medical Systems, Milwaukee, Wis) were performed according to a standard departmental protocol: 1:1 pitch from the lung apices through the adrenal glands, with either 5-mm collimation (eight studies) or 10-mm collimation with 5-mm collimation through the hila (eight studies). Reconstruction intervals were 10 and 5 mm for imaging performed with 10- and 5-mm collimation, respectively. Of the 16 studies, eight were performed with intravenous administration of contrast material (Oxilan; Cook, Bloomington, Ind) and eight were performed without contrast material. Images were acquired with a 512 x 512 matrix and quantized with 16 bits. The CT data were transferred in the digital imaging and communications in medicine (DICOM) format to the computer on which the nodule detection computer system was implemented. A DICOM reader (ALICE, version 4.0; Hayden Image Processing Group, Parexel International, Boulder, Colo) was used to translate the CT data from DICOM format into binary data format.
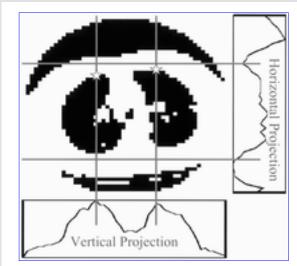
Radiologist Analysis

One thoracic radiologist (J.P.K.), without knowledge of the results of the computer system, evaluated the CT scans for nodules. To maximize nodule detection, initial and follow-up scans were evaluated concurrently by using a clinical picture archiving and communication system workstation (Impax; Agfa, Ridgefield Park, NJ) with a 12-bit display. Nodules were identified and labeled on the hard copies of each CT study. Normal structures that were believed to simulate nodules were not marked. The radiologist noted nodule development, increase, stability, decrease, or resolution that occurred between the initial and follow-up studies. The radiologist estimated change visually unless there was uncertainty, at which point electronic calipers were used for clarification, particularly when studies were acquired with different fields of view. Nodules that were adjacent to a vessel or lung border were identified.

Computer Vision System

The computer vision system we developed was implemented on a personal computer (Dimension XPS, Dell Computer, Round Rock, Tex; LINUX version 5.2, Red Hat, Durham, NC; Pentium II, Intel, Phoenix, Ariz). A computer vision system is a collection of computer programs that performs automated analysis of image data (13).

Thorax and lung border detection.—Hounsfield units for attenuation were translated into brightness values during conversion into DICOM format. Thresholding of each CT image was performed to create a binary image. The higher attenuation soft tissue and bones were visible as bright gray values, whereas the lower attenuation air-filled lung parenchyma was visible as dark gray values. The thorax was detected by means of analysis of vertical and horizontal profiles of the binary image (Fig 1a). These profiles were used to identify an initial point on the lung border. Beginning at this point, the border was traced with a method based on a backtracking algorithm (14) that detected and bridged narrow channels that were vessels or artifacts. These channels were included in the lung parenchyma.
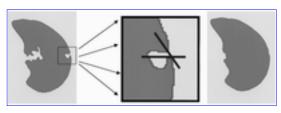

View larger version (53K):
[in this window]
[in a new window]

Figure 1a. Demonstration of thorax and lung border detection. **(a)** Computer-generated binary image of the thorax is shown with its horizontal and vertical projection histograms, which are used to determine initial lung border points (☆) to begin tracing of the lung border. **(b)** Diagram demonstrates border correction. A nodule that touches the lung border is initially excluded from the lung parenchyma. Border correction is performed by comparing the curvatures at points on the lung border, and the lung nodule is then included in the lung parenchyma. **(c)** On a chest CT image, the lung border is traced. The pixels of both lungs are used to calculate the main centroid (white cross marked *M*), whereas the pixels of the individual lungs are used to calculate the respective right and left lung centroids (white crosses labeled *R* and *L*). The black crosses indicate the most anterior, posterior, lateral, and medial pixels of each lung. Candidate regions detected by the computer that represent either nodule or normal structures are identified.
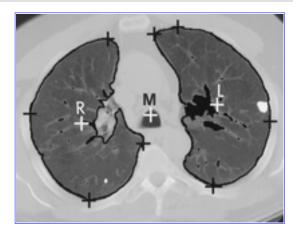
View larger version (31K):
[in this window]
[in a new window]

Figure 1b. Demonstration of thorax and lung border detection. **(a)** Computer-generated binary image of the thorax is shown with its horizontal and vertical projection histograms, which are used to determine initial lung border points (☆) to begin tracing of the lung border. **(b)** Diagram demonstrates border correction. A nodule that touches the lung border is initially excluded from the lung parenchyma. Border correction is performed by comparing the curvatures at points on the lung border, and the lung nodule is then included in the lung parenchyma. **(c)** On a chest CT image, the lung border is traced. The pixels of both lungs are used to calculate the main centroid (white cross marked M), whereas the pixels of the individual lungs are used to calculate the respective right and left lung centroids (white crosses labeled R and L). The black crosses indicate the most anterior, posterior, lateral, and medial pixels of each lung. Candidate regions detected by the computer that represent either nodule or normal structures are identified.

View larger version (118K):
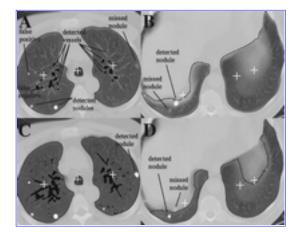[in this window]
[in a new window]

Figure 1c. Demonstration of thorax and lung border detection. **(a)** Computer-generated binary image of the thorax is shown with its horizontal and vertical projection histograms, which are used to determine initial lung border points (☆) to begin tracing of the lung border. **(b)** Diagram demonstrates border correction. A nodule that touches the lung border is initially excluded from the lung parenchyma. Border correction is performed by comparing the curvatures at points on the lung border, and the lung nodule is then included in the lung parenchyma. **(c)** On a chest CT image, the lung border is traced. The pixels of both lungs are used to calculate the main centroid (white cross marked M), whereas the pixels of the individual lungs are used to calculate the respective right and left lung centroids (white crosses labeled R and L). The black crosses indicate the most anterior, posterior, lateral, and medial pixels of each lung. Candidate regions detected by the computer that represent either nodule or normal structures are identified.

Lung border correction and parenchymal detection.—The computer system occasionally excluded from

the lung parenchyma any nodules that contacted the lung border. The computer system identified when this occurred by comparing the curvatures at points on the lung border. A rapid change in curvature indicated a nodule, large vessel, or bronchus that formed an acute or obtuse angle with the lung border, and the lung border was then corrected by means of insertion of a border segment (Fig 1b).

The centroid of an area was defined as the central balance point for the area. The centroids for the individual right and left lungs were calculated on the basis of the number and locations of pixels in the parenchyma of the right and left lungs, respectively (Fig 1c). The number and locations of pixels in both lungs were used to calculate the main centroid.

Determination of candidate regions.—The pixels in the lung parenchyma were divided into two subsets: a brighter subset, which related to normal structures (vessels, bronchi) and lung pathologic conditions (nodules), and a darker subset, which reflected the aerated lung. Structures that filled the entire section thickness appeared brighter than structures that were smaller than the section thickness, because the latter were averaged with the surrounding lung. To find nodules that were smaller than the section thickness, several gray-level thresholds were applied to create binary images that contained different candidate regions (Fig 2). The sequential labeling algorithm described by Horn (13) distinguishes and labels the candidate regions.
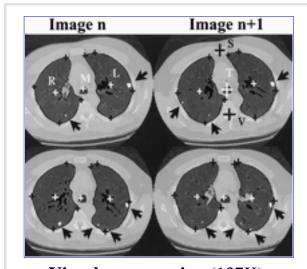

Figure 2. CT images illustrate the use of high (*A*, *B*) and low (*C*, *D*) gray-level thresholds to process images and identify candidate regions. Centroids (crosses) of the left and right lungs and the main lung are shown. Detected vessels are black, and detected nodules are white. In *A*, the nodule in the periphery of the left upper lobe was not detected with a higher threshold, but it was detected in *C* with a lower threshold.

View larger version (130K):
[in this window]
[in a new window]

Computation of properties of candidate regions.—Candidate regions were analyzed in terms of location and shape to differentiate between the normal structures (vessels, bronchi) and nodules (Fig 2). The number of pixels in each candidate region was computed as a first estimate of the two-dimensional transverse area. This estimate was used to compute the centroid of the region. The distance of this regional centroid to the ipsilateral lung centroid and the medial and lateral lung borders was computed. Each lung in each image was segmented into five regions, with specific distance criteria applied. Because vessels are typically not seen at CT within 5 mm of the pleura, large candidate regions close to the border

of the lung were determined to be "likely nodules."

Shape determination was performed with two methods to characterize candidate regions as either nodules, which are circular, or vessels, which are elongated. However, circular regions on CT images may also be vessels in cross section. Lines of pixels for which the sum E of the square of the distance to points in the region were a minimum (E_{min}) and maximum (E_{max}) were automatically identified for each candidate region. The ratio E_{min}/E_{max} was 0 for a straight-line region and 1 for a circular region; therefore, the ratio is an indicator of how elongated or circular the region is. The second measure of shape made use of a circle surrounding the candidate region. A rounder candidate region occupied a larger percentage of pixels in the circle than did an elongated candidate region.

Analysis of consecutive CT sections with three-dimensional techniques.—The CT matrix location of a nodule centroid in one image was used as an estimate for the position of the projected nodule centroid in the subsequent image. A fixed area of 10^2 pixels around this projected centroid was searched automatically to locate the centroid of a corresponding nodule. On images that depicted the trachea, the centroids of the trachea were calculated and registered to align consecutive images in the same study. Small differences in the positions of tracheal centroids were used to adjust the search area for a corresponding nodule (Fig 3).

View larger version (137K):
[in this window]
[in a new window]

Figure 3. CT images illustrate automated registration techniques for study 1 (top row) and study 2 (bottom row). The computer aligns consecutive images (*Image n* and *Image n + 1*) and detects nodules (arrows) in the same study. Images and nodules in study 1 are then matched with those in study 2. The thorax is rotated to the right in study 1 and mildly rotated to the left in study 2. Various centroids are used to detect and adjust for differences in torso rotation and translation. Centroids of the sternum (black cross marked with *S*), thoracic vertebra (black cross marked with *V*), trachea (white cross marked with *T*), both lungs (white cross marked with *M*), right lung (white cross marked with *R*), and left lung (white cross marked with *L*) are shown. The most medial, lateral, anterior, and posterior pixels on each lung are also used for registration. These pixels are marked with black crosses. Detected vessels are black.

The volume of a nodule was calculated after automatic identification of the image in which the nodule was brightest. The nodule diameter (*d*) was measured in pixels and then translated into millimeters by dividing the width of the field of view by the width of the matrix (512). Assuming that a nodule has a spherical shape, the volume of a nodule was calculated with the formula $4/3\pi(d/2)^3$ and expressed in cubic millimeters.

Analysis of change over time.—Identification of corresponding nodules on separate studies was more challenging than was identification of corresponding nodules on consecutive images in the same study. Differences in patient position and inspiration complicated registration between two different CT studies.

For each image in a patient's initial CT study, the computer identified a possible matching image and two surrounding images in the follow-up CT study. This was performed with use of centroids of anatomic structures such as the sternum, vertebra, and trachea ([Fig 3](#)). By aligning anatomic centroids, differences in translation and rotation could be addressed. The centroid of the trachea was used because the trachea is typically a midline structure. However, the trachea can be shifted secondary to atelectasis or an adjacent mass and may not be a consistent landmark for registration. The most medial, lateral, anterior, and posterior pixels of each lung were also identified and registered as were the centroids of the individual and combined lungs. Results of global registration were used to quantify the translational and rotational differences between images. Given the centroid of a nodule in one image, a projected centroid of the same nodule in an image from a subsequent study was calculated with the translational and rotational parameters generated from the global registration of thoracic structures. A fixed area of 10^2 pixels around this projected centroid was searched to locate the centroid of the corresponding nodule. The initial study was similarly searched to identify nodules that corresponded with nodules identified on the follow-up study. The sizes of corresponding nodules in the two studies were then compared.

With the computer vision system used in this study, the lung apices needed to be identified manually on all studies. The computer system then searched for corresponding images between the two studies. In all patients, human intervention was needed to match studies obtained with differing section thickness and large variations in patient inspiration and to resolve ambiguities when the search in the local neighborhood resulted in identification of more than one possible corresponding nodule.

Computer Analysis of Data

The computer vision system analyzed each study and applied rule-based classification tests to identify "highly likely nodules," "likely nodules," and "normal structures." Results by the computer were compared with those by the radiologist. A Student *t* test was performed (EXCEL; Microsoft, Redmond, Wash) to identify any differences in nodule detection rates between CT studies performed with and those performed without intravenous contrast material. The computer system measured the diameters of both detected and missed nodules and placed nodules into three size categories. The categories, which were based on findings with pulmonary nodules at low-dose CT ([4](#)), were large (>10 mm), medium ($\geq$5 mm, $\leq$10 mm), or small (<5 mm). The number of nodules in each category was counted, and the mean nodule size for each category and the entire study was tabulated.

The imaging computer system compared two sequential studies from the same patient and estimated changes in the size of a nodule by assessing for a change in size category. The relationship of assessments of nodule change by the computer and by the radiologist was determined with the Spearman rank correlation coefficient ([15](#)) (software, SAS, SAS Institute, Cary, NC; computer, Hewlett Packard, Palo Alto, Calif).

▶ Results

In the 16 chest CT studies in the eight patients, the thoracic radiologist identified 370 nodules and the computer identified 318 (86%) (Table 1). Twenty-four (46%) of the 52 missed nodules were 3 mm or less in diameter. Thirty-eight (73%) of the missed nodules were small, 12 (23%) were medium, and two (4%) were large. Thirty (58%) of the missed nodules contacted the lung border, and 13 (25%) were adjacent to a vessel.

View this table: [in this window] [in a new window]	TABLE 1. Assessment of Nodules by Computer and Thoracic Radiologist

After eliminating all nodules with a diameter of 3 mm or less, the imaging computer system detected 267 (91%) of 295 nodules: A1, 91% (43 of 47); A2, 90% (37 of 41); B1, 100% (10 of 10); B2, 100% (10 of 10); C1, 92% (11 of 12); C2, 100% (10 of 10); D1, 83% (30 of 36); D2, 94% (80 of 85); E1, 100% (four of four); E2, 100% (three of three); F1, 71% (five of seven); F2, 75% (six of eight); G1, 75% (six of eight); G2, 80% (eight of 10); H1, 100% (two of two); and H2, 100% (two of two).

On average, 76 candidate regions were classified for each image, and 3% (2.3 of 76) of these regions were misclassified as nodules on the basis of the threshold used. On average, 4.8% (12 of 252) of the candidate regions were misclassified with lower thresholds, and 3% (one of 33) were misclassified with higher thresholds. Nodule detection rates were 86% (199 of 230 nodules) for the eight nonenhanced studies and 85% (121 of 142) for the eight contrast-enhanced studies (difference not significant [$P = .91$]). Table 2 summarizes the size analysis with the computer. Sixty (16.2%) of the nodules were large; 123 (33.2%), medium; and 187 (50.5%), small (range, 0.7 mm to 3.6 cm).

View this table: [in this window] [in a new window]	TABLE 2. Computer Analysis of Nodule Size

Assessment of nodule change was correlated between the radiologist and the computer (Spearman rank correlation coefficient, 0.932) (Fig 4). Both the radiologist and computer determined that the majority of nodules increased in patients B and D and remained stable in patients C, E, and F. In patient G, the radiologist determined nine nodules were stable and seven increased, and the computer determined eight were stable and eight increased. Disease progressed clinically in patients B, D, and G and was stable in patients C, E, and F. In patient H, whose disease improved in the abdomen, the computer and radiologist

determined equal numbers of nodules were stable, increased, or decreased. For patient A, the radiologist determined that a majority of nodules decreased, which matched the patient's clinical course, whereas the computer determined that a majority remained stable.
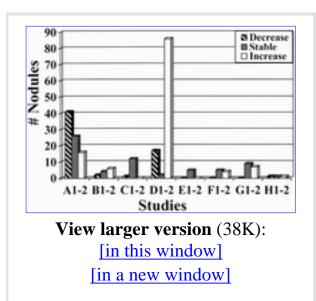

Figure 4a. Bar graphs depict results of assessment of overall change in nodules by the **(a)** radiologist and **(b)** computer. Results for change in the majority of nodules were similar in six patients.

View larger version (38K):
[in this window]
[in a new window]

Figure 4b. Bar graphs depict results of assessment of overall change in nodules by the **(a)** radiologist and **(b)** computer. Results for change in the majority of nodules were similar in six patients.
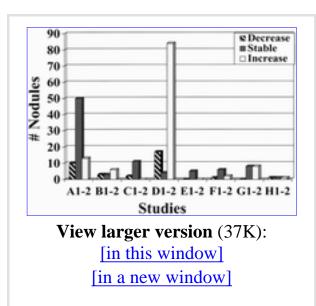
View larger version (37K):
[in this window]
[in a new window]

▶ Discussion

Our research resulted in development of algorithms for thorax and lung detection, a rule-based classification method for nodule detection, procedures for lung and nodule registration, and techniques for assessment of nodule change over time.

Although our computer system is still preliminary, our results for nodule detection are promising. The computer system identified 86% of all nodules and 91% of nodules larger than 3 mm. The missed nodules were predominantly smaller than 3 mm or contacted the lung border. To ensure that nodules abutting the lung border were not unintentionally excluded from the lung parenchyma, the computer system automatically analyzed the curvature of points along the lung border and inserted border segments into high-curvature portions of the border. The computer systems of Kanazawa et al ([3]) and Armato et al ([2]) also insert border segments when high-curvature points are detected. The system of Armato et al detects high-curvature points when a disk rolled along the initially detected border contacts the border at two points rather than one.

A computer system with the ability to register thoracic CT images between different studies has not been previously reported, to our knowledge. We have developed registration techniques and combined them with automated nodule recognition techniques to identify nodules on two studies and compare them.

Registration of studies is challenging owing to differences in rotation and translation of the imaged structures. Additional difficulties arise in the registration of thoracic images as a result of differences in patient inspiration. The radiology literature reports many registration techniques for the brain and other organ systems. For example, positron emission tomography (PET) has been correlated with magnetic resonance (MR) imaging for the brain ([16]–[19]). Nuclear medicine bone scans have been registered with bone radiographs ([20]). Preliminary studies have been performed for registration of PET and CT scans in the thorax ([21]). Registration methods often require some manual input to compensate for rotational and translational differences between two studies ([16],[18]). For example, registration of PET and MR studies of the brain was aided by the manual identification of the midsagittal plane and subsequent reconstruction of the transverse images ([17]).

Our computer system accounted for differences in patient rotation and translation by computing centroids of the lungs, trachea, vertebra, and sternum. Our techniques, although not entirely automated, enable comparison of nodules in two different CT studies. Methods that automatically account for patient tilt in the craniocaudal dimension, differences in respiration, and alignment of the lung apices are challenging and need to be developed further. Our computer vision system can identify a nodule on multiple consecutive sections without human intervention if a nodule appears on more than one image in the same study. Further work will deal with the differentiation of a nodule from vertically oriented vessels.

The computer vision system automatically measured the diameter of the nodule and determined any change in nodule diameter between two studies. These measurements can be converted into volumetric values. Assuming a nodule is a sphere, a change in nodule diameter by 26% creates a doubling of nodule volume ([22]). In our study, for example, a spherical nodule had a diameter of six pixels, which translated into a diameter of 4.5 mm and a volume of 47.7 mm^3. The computer vision system then detected the same nodule on the follow-up study and measured the diameter as seven pixels, or 5.25 mm. The volume was calculated as 75.7 mm^3, which was a 62% increase. This example illustrates that a one-pixel difference in diameter translates into a large change in volume.

A one-pixel difference is difficult for a radiologist to ascertain; therefore, it is desirable for a computer system to automatically identify such a small pixel change. The one-pixel difference may not be due to a change in volume but may be secondary to sampling inaccuracies. Measurement of the apparent nodule size by the computer system is affected by the threshold values for pixel intensities that are used to distinguish brighter soft-tissue structures from the darker air-containing components of the lung. The CT scanner, kilovolt potential, reconstruction algorithm, section thickness, and nodule location in the field of view have been shown to affect pixel intensity (23) and, therefore, apparent nodule diameter. Further studies are needed to establish statistical bounds on the estimation error of change-in-diameter measurements. To avoid potential sampling errors in this preliminary study, we reported the change in nodule size determined by the computer in terms of change in size category. Although assessments of nodule change by the computer and radiologist correlated well with our choice of categories, a small decrease in nodule size may not have satisfied the criteria for change in category for the computer and therefore may account for some differences.

As in other preliminary studies (3,5), true- and false-positive rates reported in this study were computed for data that were used to develop the classification rules of the computer vision system. In the future, we will create a substantially larger database and separate it into training and test cases. Nodules in the training cases will be analyzed to improve the classification rules, and computer system efficacy will be assessed with test cases only and with more than one radiologist.

The computer vision system used in this study has quantitative abilities that could affect many facets of oncology care, from diagnosis of metastases to assessment of their response to chemotherapy. In the future, low-dose chest CT could be used for lung cancer screening. Use of this vision system could help ensure that nodules do not fail to be detected. In screening mammography, computer systems have been shown to improve receiver operating characteristic curves of radiologists for rating the likelihood of malignancy (24) and detecting abnormalities (25). Computer-aided diagnostic imaging systems that interact with a radiologist by means of an interface are being developed in mammography (26). Such an interface could easily be added to this computer vision system and would have many applications in thoracic radiology.

Our preliminary computer vision system demonstrates the potential for a clinically useful automated nodule detection system that quantifies nodule size and assesses for change over time. With further development, such a computer system could be applied to clinical scenarios in which objective nodule assessment is necessary.

▶ ACKNOWLEDGMENTS

▶ FOOTNOTES

Abbreviation: DICOM = digital imaging and communications in medicine

Author contributions: Guarantors of integrity of entire study, J.P.K., M.B.; study concepts and design, J.P.K., M.B.; definition of intellectual content, J.P.K., M.B.; literature research, J.P.K., M.B.; experimental studies, J.P.K., M.B.; data acquisition, J.P.K., M.B.; data analysis, J.P.K., M.B.; statistical analysis, J.P.K., M.B.; manuscript preparation, editing, and review, J.P.K., M.B.

▶ REFERENCES

1. Landis SH, Murray T, Bolden S, Wingo PA. Cancer statistics, 1999. CA Cancer J Clin 1999; 49:8-31.[Medline]

2. Armato SG, III, Giger ML, Moran CJ, Blackburn JT, Doi K, MacMahon H. Computerized detection of pulmonary nodules on CT scans. RadioGraphics 1999; 19:1303-1311.[Abstract/Full Text]

3. Kanazawa K, Kawata Y, Niki N, et al. Computer-aided diagnosis for pulmonary nodules based on helical CT images. Comput Med Imaging Graph 1998; 22:157-167.[Medline]

4. Henschke CI, Yankelevitz DF, Mateescu I, Brettle DW, Rainey TG, Weingard FS. Neural networks for the analysis of small pulmonary nodules. Clin Imaging 1997; 21:390-399.[Medline]

5. Giger ML, Bae KT, MacMahon H. Computerized detection of pulmonary nodules in computed tomography images. Invest Radiol 1994; 29:459-465.[Medline]

6. Matsumoto T, Yoshimura H, Giger ML, et al. Potential usefulness of computerized nodule detection in screening programs for lung cancer. Invest Radiol 1992; 27:471-475.[Medline]

7. Xu XW, Doi K, Kobayashi T, MacMahon H, Giger ML. Development of an improved CAD scheme for automated detection of lung nodules in digital chest images. Med Phys 1997; 24:1395-1403.[Medline]

8. MacMahon H, Engelmann R, Behlen FM, et al. Computer-aided diagnosis of pulmonary nodules: results of a large-scale observer test. Radiology 1999; 213:723-726.[Abstract/Full Text]

9. Ashizawa K, MacMahon H, Ishida T, et al. Effect of an artificial neural network on radiologists' performance in the differential diagnosis of interstitial lung disease with chest radiographs. AJR Am J Roentgenol 1999; 172:1311-1315.[Abstract]

10. Yankelevitz DF, Gupta R, Zhao B, Henschke CI. Small pulmonary

nodules: evaluation with repeat CT—preliminary experience. Radiology 1999; 212:561-566.[Abstract/Full Text]

11. Henschke CI, McCauley DI, Yankelevitz DF, et al. Early lung cancer action project: overall design and findings from baseline screening. Lancet 1999; 354:99-105.[Medline]

12. Kakinuma R, Ohmatsu H, Kaneko M, et al. Detection failures in spiral CT screening for lung cancer: analysis of CT findings. Radiology 1999; 212:61-66.[Abstract/Full Text]

13. Horn BKP. Robot vision Cambridge, Mass: MIT Press, 1986; 69-71.

14. Wirth N. Algorithmen und datenstrukturen Stuttgart, Germany: Teubner, 1983; 162-185.

15. Rosner B. Fundamentals of biostatistics 3rd ed. Belmont, Calif: Duxbury, 1990; 450-455.

16. Kapouleas I, Alavi A, Alves WM, Gur RE, Weiss DW. Registration of three-dimensional MR and PET images of the human brain without markers. Radiology 1991; 181:731-739.[Abstract]

17. Uematsu H, Sadato N, Yonekura Y, et al. Coregistration of FDG PET and MRI of the head and neck using normal distribution of FDG. J Nucl Med 1998; 39:2121-2127.[Medline]

18. Pelizzari CA, Chen GT, Spelbring DR, Weichselbaum RR, Chen CT. Accurate three-dimensional registration of CT, PET, and/or MR images of the brain. J Comput Assist Tomogr 1989; 13:20-26.[Medline]

19. Turkington TG, Jaszczak RJ, Pelizzari CA, et al. Accuracy of registration of PET, SPECT and MR images of a brain phantom. J Nucl Med 1993; 34:1587-1594.[Medline]

20. Robinson AH, Bird N, Screaton N, Wraight EP, Meggitt BF. Coregistration imaging of the foot: a new localisation technique. J Bone Joint Surg Br 1998; 80:777-780.[Medline]

21. Yu JN, Fahey FH, Gage HD, et al. Intermodality, retrospective image registration in the thorax. J Nucl Med 1995; 36:2333-2338.[Medline]

22. Naidich DP, Webb WR, Muller NL, Krinsky GA, Zerhouni EA, Siegelman SS. Focal lung disease. Computed tomography and magnetic resonance of the thorax 3rd ed. Philadelphia, Pa: Lippincott-Raven, 1999; 313.

23. Zerhouni EA, Spivey JF, Morgan RH, Leo FP, Stitik FP, Siegelman SS. Factors influencing quantitative CT measurements of solitary pulmonary nodules. J Comput Assist Tomogr 1982; 6:1075-1087.[Medline]

24. Chan HP, Sahiner B, Helvie MA, et al. Improvement of radiologists' characterization of mammographic masses by using computer-aided

diagnosis: an ROC study. Radiology 1999; 212:817-827.[Abstract/Full Text]

25. Chan HP, Doi K, Vyborny CJ, et al. Improvement of radiologists' detection of clustered microcalcifications on mammograms: the potential of computer-aided diagnosis. Invest Radiol 1990; 25:1102-1110.[Medline]

26. Giger M, MacMahon H. Image processing and computer-aided diagnosis. Radiol Clin North Am 1996; 34:565-596.[Medline]

▶ Abstract of this Article
▶ Figures Only for this Article
▶ **Reprint (PDF) Version of this Article**
▶ **eLetters: Submit a response to this article**
▶ Similar articles found in:
　　Radiology Online
▶ Search Medline for articles by:
　　Ko, J. P. || Betke, M.
▶ Alert me when:
　　new articles cite this article

| HOME | HELP | FEEDBACK | SUBSCRIPTIONS | ARCHIVE | SEARCH | TABLE OF CONTENTS |

| RADIOLOGY | RADIOGRAPHICS | RSNA JOURNALS ONLINE |

Radiology

HOME **HELP** **FEEDBACK** **SUBSCRIPTIONS** **ARCHIVE** **SEARCH** **TABLE OF CONTENTS**

Institution: NYU Medical Center || **Sign In as Member** || **Contact Subscription Administrator at this Site** || **FAQ**

Reprint (PDF) Version

Download

the Reprint (PDF)
version of:
Radiology Ko and Betke 218
(1): 267. **(682K)**

- **Abstract of this Article**
- **Figures Only for this Article**
- **Full Text (HTML) of this Article**
- **eLetters: Submit a response to this article**
- Similar articles found in:
  Radiology Online
- Search Medline for articles by:
  Ko, J. P. || **Betke, M.**
- Alert me when:
  new articles cite this article

This file is in Adobe Acrobat (PDF) format. If you have not installed and configured the Adobe Acrobat Reader on your system, please see **Help with Printing** for instructions.

Having trouble reading a PDF online?

PDFs are designed to be printed out and read, but if you prefer to read them online, you may find it easier if you increase the view size to 125%.

Having trouble printing a PDF?

1. **Try printing one page at a time.**
2. **Try printing with the 'Print as Image' option selected.**
3. **Try printing to a newer printer.** (NOTE for Macintosh users: A number of users have reported problems printing PDFs with the LaserWriter Driver version 8.4. We suggest using an earlier or later version.)
4. **Try saving the file to disk before printing** rather than opening it "on the fly." This requires that you configure your browser to "Save" rather than "Launch Application" for the file type "application/pdf," and can usually be done in the "Helper Applications" options.
5. **Make sure you are using the latest version of Adobe's Acrobat Reader.** See **Help with Printing** for details.
6. **Are you getting Postscript errors on your Mac?** A frequent cause is a lack of communication of postscript commands between your computer and your printer. Postscript communication on a Mac is handled by the Control Panel called ~ATM. To see if you have installed ~ATM, go to the `System Folder / Control Panels` folder and look for ~ATM. If the control panel is not present you will need to install it. If the ~ATM is installed, please check to make sure that you are using the most recent version, v4.0 or higher. You can check the version number by selecting the ~ATM icon and choosing `Get info...` from the `File` menu.

If you do not have ~ATM installed or need to upgrade to the latest version, you can get this software from the [Acrobat web site](). If you recently downloaded Acrobat, you may already have this Control Panel on your computer and just need to install it. When you download Acrobat, ~ATM comes along in a folder called Fonts and will be located in the Acrobat folder. Drag the ~ATM icon onto your System Folder to install it.

7. **Are some lines on each page getting cut off?**
   Are you running MacOS version 8? The default paper size is "Letter Small." Change this setting to "US Letter" in File/Page Setup and you should be able to print full pages.

8. **If the file is taking more than 15 minutes to download**, please see [Tips for users experiencing slow response]().

9. **More Questions?** See [Frequently Asked Questions about PDFs]()

Jane P. Ko, MD
Margrit Betke, PhD

Author contributions:
Guarantors of integrity of entire study, J.P.K., M.B.; study concepts and design, J.P.K., M.B.; definition of intellectual content, J.P.K., M.B.; literature research, J.P.K., M.B.; experimental studies, J.P.K., M.B.; data acquisition, J.P.K., M.B.; data analysis, J.P.K., M.B.; statistical analysis, J.P.K., M.B.; manuscript preparation, editing, and review, J.P.K., M.B.

Chest CT: Automated Nodule Detection and Assessment of Change over Time— Preliminary Experience[1]

The authors developed a computer system that automatically identifies nodules at chest computed tomography, quantifies their diameter, and assesses for change in size at follow-up. The automated nodule detection system identified 318 (86%) of 370 nodules in 16 studies (eight initial and eight follow-up studies) obtained in eight oncology patients with known nodules. Assessment of change in nodule size by the computer matched that by the thoracic radiologist (Spearman rank correlation coefficient, 0.932).

In the United States, about 8 million people have a history of cancer, either cured or in the process of being treated, and predictions indicated that 1.2 million new diagnoses of invasive cancer would be made in 1999 (1). Extrathoracic and thoracic malignancies frequently metastasize to the lung parenchyma as pulmonary nodules, and the most sensitive diagnostic imaging modality for detecting such nodules is computed tomography (CT) of the thorax. To assess disease progression or regression with therapy when metastatic disease to the lung is discovered, precise quantitative and reproducible analysis is required of what is often a large number of nodules. Computer schemes are therefore needed that help (*a*) improve nodule detection by the radiologist, (*b*) quantify nodule volume and number, and (*c*) assess change in nodule number and diameter.

To our knowledge, research about automated assessment of change in nodule number and size has not been performed previously. Studies have primarily addressed automated nodule detection at CT (2–5) and chest radiography (6,7).

Findings demonstrate that computer-aided diagnosis systems help improve a radiologist's receiver operating characteristic curve for detecting pulmonary nodules (8) and characterizing interstitial lung disease (9) on chest radiographs. However, there is a need to better quantify the size of pulmonary nodules and their change over time. To estimate change in nodule volume, the radiologist typically uses bidimensional measurements in the transverse plane. These measurements are subject to inter- and intraobserver variations, which can be decreased with a computer system. Yankelevitz et al (10) demonstrate that growth in malignant tumors as small as 5 mm can be detected at early repeat CT with use of a semiautomated method.

A computer system for automated nodule detection and quantification capabilities could be applied to a high-volume screening scenario such as low-dose CT, which has been studied as a screening test for lung cancer in a high-risk population (11). The failure to identify a nodule at low-dose CT (12) may crucially affect a patient's prognosis, and a vision system could help decrease the number of missed nodules.

Given the potential applications to treatment and screening of patients with cancer, we developed a computer vision system that not only detects pulmonary nodules at CT but also quantifies their volume and change over time. The purpose of this study was to evaluate the performance of the computer vision system.

▮ Materials and Methods

Patient Data

Eight patients with cancer diagnoses and pulmonary nodules were selected from the patients who underwent thoracic CT at Massachusetts Hospi-

Figure 1. Demonstration of thorax and lung border detection. **(a)** Computer-generated binary image of the thorax is shown with its horizontal and vertical projection histograms, which are used to determine initial lung border points (☆) to begin tracing of the lung border. **(b)** Diagram demonstrates border correction. A nodule that touches the lung border is initially excluded from the lung parenchyma. Border correction is performed by comparing the curvatures at points on the lung border, and the lung nodule is then included in the lung parenchyma. **(c)** On a chest CT image, the lung border is traced. The pixels of both lungs are used to calculate the main centroid (white cross marked *M*), whereas the pixels of the individual lungs are used to calculate the respective right and left lung centroids (white crosses labeled *R* and *L*). The black crosses indicate the most anterior, posterior, lateral, and medial pixels of each lung. Candidate regions detected by the computer that represent either nodule or normal structures are identified.

tal (Boston) for clinical indications from January 1998 through August 1999. To select patients, we used a computer program (FOLIOVIEWS, version 3.1; InfoArchiText, Newton, Mass) that searched radiology reports of chest CT scans for the terms "pulmonary nodules" and "cancer." Patient reports were selected at random from search results. A patient was excluded if the reports included the terms "lung cancer," "consolidation," or "collapse," or if the patient did not undergo follow-up CT at our institution. This process was repeated until eight patients with 16 studies (eight initial and eight follow-up studies) were selected. The cases of the patients were labeled with a letter A through H followed by either a 1 or 2 to represent the initial or follow-up CT study, respectively. The time interval between the two CT studies was 5 ($n = 1$), 2.5 ($n = 1$), 2.25 ($n = 2$), 2 ($n = 1$), and 1.5 ($n = 3$) months. Each patient's clinical course and diagnosis was confirmed by means of chart review. Patient diagnoses were renal ($n = 1$), esophageal ($n = 1$), neuroendocrine ($n = 1$), colorectal ($n = 2$), and bladder ($n = 1$) carcinomas, as well as melanoma ($n = 1$) and sarcoma ($n = 1$).

The chest helical CT studies (HiSpeed Advantage; GE Medical Systems, Milwaukee, Wis) were performed according to a standard departmental protocol: 1:1 pitch from the lung apices through the adrenal glands, with either 5-mm collimation (eight studies) or 10-mm collimation with 5-mm collimation through the hila (eight studies). Reconstruction intervals were 10 and 5 mm for imaging performed with 10- and 5-mm collimation, respectively. Of the 16 studies, eight were performed with intravenous administration of contrast material (Oxilan; Cook, Bloomington, Ind) and eight were performed without contrast material. Images were acquired with a 512 × 512 matrix and quantized with 16 bits. The CT data were transferred in the digital im-

aging and communications in medicine (DICOM) format to the computer on which the nodule detection computer system was implemented. A DICOM reader (ALICE, version 4.0; Hayden Image Processing Group, Parexel International, Boulder, Colo) was used to translate the CT data from DICOM format into binary data format.

Radiologist Analysis

One thoracic radiologist (J.P.K.), without knowledge of the results of the computer system, evaluated the CT scans for nodules. To maximize nodule detection, initial and follow-up scans were evaluated concurrently by using a clinical picture archiving and communication sys-
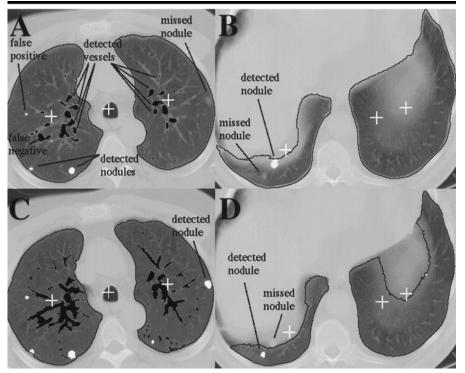
Figure 2. CT images illustrate the use of high (*A*, *B*) and low (*C*, *D*) gray-level thresholds to process images and identify candidate regions. Centroids (crosses) of the left and right lungs and the main lung are shown. Detected vessels are black, and detected nodules are white. In *A*, the nodule in the periphery of the left upper lobe was not detected with a higher threshold, but it was detected in *C* with a lower threshold.

tem workstation (Impax; Agfa, Ridgefield Park, NJ) with a 12-bit display. Nodules were identified and labeled on the hard copies of each CT study. Normal structures that were believed to simulate nodules were not marked. The radiologist noted nodule development, increase, stability, decrease, or resolution that occurred between the initial and follow-up studies. The radiologist estimated change visually unless there was uncertainty, at which point electronic calipers were used for clarification, particularly when studies were acquired with different fields of view. Nodules that were adjacent to a vessel or lung border were identified.

Computer Vision System

The computer vision system we developed was implemented on a personal computer (Dimension XPS, Dell Computer, Round Rock, Tex; LINUX version 5.2, Red Hat, Durham, NC; Pentium II, Intel, Phoenix, Ariz). A computer vision system is a collection of computer programs that performs automated analysis of image data (13).

Thorax and lung border detection.—Hounsfield units for attenuation were translated into brightness values during conversion into DICOM format. Thresholding of each CT image was performed to create a binary image. The higher attenuation soft tissue and bones were visible as bright gray values, whereas the lower attenuation air-filled lung parenchyma was visible as dark gray values. The thorax was detected by means of analysis of vertical and horizontal profiles of the binary image (Fig 1a). These profiles were used to identify an initial point on the lung border. Beginning at this point, the border was traced with a method based on a backtracking algorithm (14) that detected and bridged narrow channels that were vessels or artifacts. These channels were included in the lung parenchyma.

Lung border correction and parenchymal detection.—The computer system occasionally excluded from the lung parenchyma any nodules that contacted the lung border. The computer system identified when this occurred by comparing the curvatures at points on the lung border. A rapid change in curvature indicated a nodule, large vessel, or bronchus that formed an acute or obtuse angle with the lung border, and the lung border was then corrected by means of insertion of a border segment (Fig 1b).

The centroid of an area was defined as the central balance point for the area. The centroids for the individual right and left lungs were calculated on the basis of the number and locations of pixels in the parenchyma of the right and left lungs, respectively (Fig 1c). The number and locations of pixels in both lungs were used to calculate the main centroid.

Determination of candidate regions.—The pixels in the lung parenchyma were divided into two subsets: a brighter subset, which related to normal structures (vessels, bronchi) and lung pathologic conditions (nodules), and a darker subset, which reflected the aerated lung. Structures that filled the entire section thickness appeared brighter than structures that were smaller than the section thickness, because the latter were averaged with the surrounding lung. To find nodules that were smaller than the section thickness, several gray-level thresholds were applied to create binary images that contained different candidate regions (Fig 2). The sequential labeling algorithm described by Horn (13) distinguishes and labels the candidate regions.

Computation of properties of candidate regions.—Candidate regions were analyzed in terms of location and shape to differentiate between the normal structures (vessels, bronchi) and nodules (Fig 2). The number of pixels in each candidate region was computed as a first estimate of the two-dimensional transverse area. This estimate was used to compute the centroid of the region. The distance of this regional centroid to the ipsilateral lung centroid and the medial and lateral lung borders was computed. Each lung in each image was segmented into five regions, with specific distance criteria applied. Because vessels are typically not seen at CT within 5 mm of the pleura, large candidate regions close to the border of the lung were determined to be "likely nodules."

Shape determination was performed with two methods to characterize candidate regions as either nodules, which are circular, or vessels, which are elongated. However, circular regions on CT images may also be vessels in cross section. Lines of pixels for which the sum E of the square of the distance to points in the region were a minimum (E_{min}) and maximum (E_{max}) were automatically identified for each candidate region. The ratio E_{min}/E_{max} was 0 for a straight-line region and 1 for a circular region; therefore, the ratio is an indicator of how elongated or

circular the region is. The second measure of shape made use of a circle surrounding the candidate region. A rounder candidate region occupied a larger percentage of pixels in the circle than did an elongated candidate region.

Analysis of consecutive CT sections with three-dimensional techniques.—The CT matrix location of a nodule centroid in one image was used as an estimate for the position of the projected nodule centroid in the subsequent image. A fixed area of 10^2 pixels around this projected centroid was searched automatically to locate the centroid of a corresponding nodule. On images that depicted the trachea, the centroids of the trachea were calculated and registered to align consecutive images in the same study. Small differences in the positions of tracheal centroids were used to adjust the search area for a corresponding nodule (Fig 3).

The volume of a nodule was calculated after automatic identification of the image in which the nodule was brightest. The nodule diameter (*d*) was measured in pixels and then translated into millimeters by dividing the width of the field of view by the width of the matrix (512). Assuming that a nodule has a spherical shape, the volume of a nodule was calculated with the formula $4/3\pi(d/2)^3$ and expressed in cubic millimeters.

Analysis of change over time.—Identification of corresponding nodules on separate studies was more challenging than was identification of corresponding nodules on consecutive images in the same study. Differences in patient position and inspiration complicated registration between two different CT studies.

For each image in a patient's initial CT study, the computer identified a possible matching image and two surrounding images in the follow-up CT study. This was performed with use of centroids of anatomic structures such as the sternum, vertebra, and trachea (Fig 3). By aligning anatomic centroids, differences in translation and rotation could be addressed. The centroid of the trachea was used because the trachea is typically a midline structure. However, the trachea can be shifted secondary to atelectasis or an adjacent mass and may not be a consistent landmark for registration. The most medial, lateral, anterior, and posterior pixels of each lung were also identified and registered as were the centroids of the individual and combined lungs. Results of global registration were used to quantify the translational and rotational differences between images. Given the centroid of a nodule in one image, a pro-
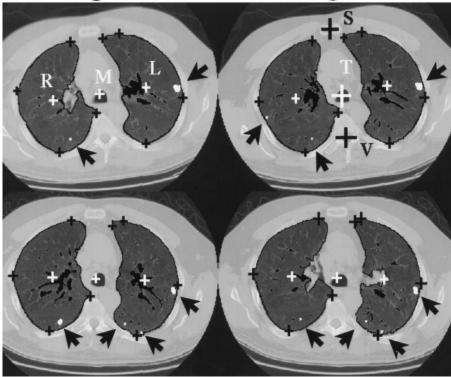

Figure 3. CT images illustrate automated registration techniques for study 1 (top row) and study 2 (bottom row). The computer aligns consecutive images (*Image n* and *Image n + 1*) and detects nodules (arrows) in the same study. Images and nodules in study 1 are then matched with those in study 2. The thorax is rotated to the right in study 1 and mildly rotated to the left in study 2. Various centroids are used to detect and adjust for differences in torso rotation and translation. Centroids of the sternum (black cross marked with *S*), thoracic vertebra (black cross marked with *V*), trachea (white cross marked with *T*), both lungs (white cross marked with *M*), right lung (white cross marked with *R*), and left lung (white cross marked with *L*) are shown. The most medial, lateral, anterior, and posterior pixels on each lung are also used for registration. These pixels are marked with black crosses. Detected vessels are black.

jected centroid of the same nodule in an image from a subsequent study was calculated with the translational and rotational parameters generated from the global registration of thoracic structures. A fixed area of 10^2 pixels around this projected centroid was searched to locate the centroid of the corresponding nodule. The initial study was similarly searched to identify nodules that corresponded with nodules identified on the follow-up study. The sizes of corresponding nodules in the two studies were then compared.

With the computer vision system used in this study, the lung apices needed to be identified manually on all studies. The computer system then searched for corresponding images between the two studies. In all patients, human intervention was needed to match studies obtained with differing section thickness and large variations in patient inspiration and to resolve ambiguities when the search in

the local neighborhood resulted in identification of more than one possible corresponding nodule.

Computer Analysis of Data

The computer vision system analyzed each study and applied rule-based classification tests to identify "highly likely nodules," "likely nodules," and "normal structures." Results by the computer were compared with those by the radiologist. A Student *t* test was performed (EXCEL; Microsoft, Redmond, Wash) to identify any differences in nodule detection rates between CT studies performed with and those performed without intravenous contrast material. The computer system measured the diameters of both detected and missed nodules and placed nodules into three size categories. The categories, which were based on findings with pulmonary nodules at low-dose CT (4), were

TABLE 1
Assessment of Nodules by Computer and Thoracic Radiologist

Patient	Study 1					Study 2				
	No. of Nodules Detected by Computer	Total No. of Nodules Detected by Radiologist	Percentage (computer no./ radiologist no.)	No. of Highly Likely Nodules	No. of Likely Nodules	No. of Nodules Detected by Computer	Total No. of Nodules Detected by Radiologist	Percentage (computer no./ radiologist no.)	No. of Highly Likely Nodules	No. of Likely Nodules
A	58	70	83	25	33	62	72	86	24	38
B	10	10	100	6	4	10	10	100	5	5
C	11	13	85	9	2	12	12	100	10	2
D	31	38	82	17	14	83	90	92	58	25
E	4	5	80	3	1	4	5	80	3	1
F	5	7	71	5	0	7	9	78	4	3
G	6	9	67	2	4	11	16	69	10	1
H	2	2	100	2	0	2	2	100	2	0

TABLE 2
Computer Analysis of Nodule Size

Patient	Study 1				Study 2			
	Large	Medium	Small	Total	Large	Medium	Small	Total
A	5 (23.1)	14 (6.7)	51 (3.2)	70 (5.3)	4 (26.3)	11 (6.8)	57 (3.2)	72 (5.0)
B	1 (15.0)	4 (8.1)	5 (3.1)	10 (6.3)	4 (14.4)	3 (8.0)	3 (3.5)	10 (8.1)
C	1 (10.1)	8 (6.4)	4 (3.5)	13 (5.8)	1 (10.5)	7 (6.7)	4 (3.8)	12 (6.1)
D	6 (13.2)	19 (7.0)	13 (3.7)	38 (6.9)	30 (13.8)	37 (6.7)	23 (3.4)	90 (8.1)
E	1 (14.5)	1 (7.9)	3 (3.5)	5 (6.6)	1 (22.0)	1 (8.0)	3 (2.9)	5 (7.7)
F	2 (29.0)	5 (6.4)	0 (0)	7 (10.6)	2 (24.4)	6 (8.2)	1 (2.5)	9 (10.8)
G	1 (17.0)	1 (6.2)	7 (3.1)	9 (5.2)	1 (17.8)	3 (6.7)	12 (3.1)	16 (5.2)
H	0	2 (5.7)	0	2 (5.7)	0	1 (7.4)	1 (3.7)	2 (5.6)

Note.—Data are the number of nodules. Numbers in parentheses are mean diameter in millimeters.

large (>10 mm), medium (≥5 mm, ≤10 mm), or small (<5 mm). The number of nodules in each category was counted, and the mean nodule size for each category and the entire study was tabulated.

The imaging computer system compared two sequential studies from the same patient and estimated changes in the size of a nodule by assessing for a change in size category. The relationship of assessments of nodule change by the computer and by the radiologist was determined with the Spearman rank correlation coefficient (15) (software, SAS, SAS Institute, Cary, NC; computer, Hewlett Packard, Palo Alto, Calif).

▌ Results

In the 16 chest CT studies in the eight patients, the thoracic radiologist identified 370 nodules and the computer identified 318 (86%) (Table 1). Twenty-four (46%) of the 52 missed nodules were 3 mm or less in diameter. Thirty-eight (73%) of the missed nodules were small, 12 (23%) were medium, and two (4%) were large. Thirty (58%) of the missed nodules contacted the lung border, and 13 (25%) were adjacent to a vessel.

After eliminating all nodules with a diameter of 3 mm or less, the imaging computer system detected 267 (91%) of 295 nodules: A1, 91% (43 of 47); A2, 90% (37 of 41); B1, 100% (10 of 10); B2, 100% (10 of 10); C1, 92% (11 of 12); C2, 100% (10 of 10); D1, 83% (30 of 36); D2, 94% (80 of 85); E1, 100% (four of four); E2, 100% (three of three); F1, 71% (five of seven); F2, 75% (six of eight); G1, 75% (six of eight); G2, 80% (eight of 10); H1, 100% (two of two); and H2, 100% (two of two).

On average, 76 candidate regions were classified for each image, and 3% (2.3 of 76) of these regions were misclassified as nodules on the basis of the threshold used. On average, 4.8% (12 of 252) of the candidate regions were misclassified with lower thresholds, and 3% (one of 33) were misclassified with higher thresholds. Nodule detection rates were 86% (199 of 230 nodules) for the eight nonenhanced studies and 85% (121 of 142) for the eight contrast-enhanced studies (difference not significant [$P = .91$]). Table 2 summarizes the size analysis with the computer. Sixty (16.2%) of the nodules were large; 123 (33.2%), medium; and 187 (50.5%), small (range, 0.7 mm to 3.6 cm).

Assessment of nodule change was correlated between the radiologist and the computer (Spearman rank correlation coefficient, 0.932) (Fig 4). Both the radiologist and computer determined that the majority of nodules increased in patients B and D and remained stable in patients C, E, and F. In patient G, the radiologist determined nine nodules were stable and seven increased, and the computer determined eight were stable and eight increased. Disease progressed clinically in patients B, D, and G and was stable in patients C, E, and F. In patient H, whose disease improved in the abdomen, the computer and radiologist determined equal numbers of nodules were stable, increased, or decreased. For patient A, the radiologist determined that a majority of nodules decreased, which matched the patient's clinical course, whereas the computer determined that a majority remained stable.

▌ Discussion

Our research resulted in development of algorithms for thorax and lung detection, a rule-based classification method for nodule detection, procedures for lung
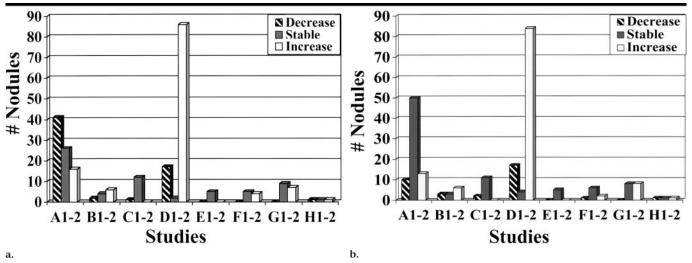
Figure 4. Bar graphs depict results of assessment of overall change in nodules by the **(a)** radiologist and **(b)** computer. Results for change in the majority of nodules were similar in six patients.

and nodule registration, and techniques for assessment of nodule change over time.

Although our computer system is still preliminary, our results for nodule detection are promising. The computer system identified 86% of all nodules and 91% of nodules larger than 3 mm. The missed nodules were predominantly smaller than 3 mm or contacted the lung border. To ensure that nodules abutting the lung border were not unintentionally excluded from the lung parenchyma, the computer system automatically analyzed the curvature of points along the lung border and inserted border segments into high-curvature portions of the border. The computer systems of Kanazawa et al (3) and Armato et al (2) also insert border segments when high-curvature points are detected. The system of Armato et al detects high-curvature points when a disk rolled along the initially detected border contacts the border at two points rather than one.

A computer system with the ability to register thoracic CT images between different studies has not been previously reported, to our knowledge. We have developed registration techniques and combined them with automated nodule recognition techniques to identify nodules on two studies and compare them.

Registration of studies is challenging owing to differences in rotation and translation of the imaged structures. Additional difficulties arise in the registration of thoracic images as a result of differences in patient inspiration. The radiology literature reports many registration techniques for the brain and other organ systems. For example, positron emission tomography (PET) has been correlated with magnetic resonance (MR) imaging for the brain (16–19). Nuclear medicine bone scans have been registered with bone radiographs (20). Preliminary studies have been performed for registration of PET and CT scans in the thorax (21). Registration methods often require some manual input to compensate for rotational and translational differences between two studies (16,18). For example, registration of PET and MR studies of the brain was aided by the manual identification of the midsagittal plane and subsequent reconstruction of the transverse images (17).

Our computer system accounted for differences in patient rotation and translation by computing centroids of the lungs, trachea, vertebra, and sternum. Our techniques, although not entirely automated, enable comparison of nodules in two different CT studies. Methods that automatically account for patient tilt in the craniocaudal dimension, differences in respiration, and alignment of the lung apices are challenging and need to be developed further. Our computer vision system can identify a nodule on multiple consecutive sections without human intervention if a nodule appears on more than one image in the same study. Further work will deal with the differentiation of a nodule from vertically oriented vessels.

The computer vision system automatically measured the diameter of the nodule and determined any change in nodule diameter between two studies. These measurements can be converted into volumetric values. Assuming a nodule is a sphere, a change in nodule diameter by 26% creates a doubling of nodule volume (22). In our study, for example, a spherical nodule had a diameter of six pixels, which translated into a diameter of 4.5 mm and a volume of 47.7 mm^3. The computer vision system then detected the same nodule on the follow-up study and measured the diameter as seven pixels, or 5.25 mm. The volume was calculated as 75.7 mm^3, which was a 62% increase. This example illustrates that a one-pixel difference in diameter translates into a large change in volume.

A one-pixel difference is difficult for a radiologist to ascertain; therefore, it is desirable for a computer system to automatically identify such a small pixel change. The one-pixel difference may not be due to a change in volume but may be secondary to sampling inaccuracies. Measurement of the apparent nodule size by the computer system is affected by the threshold values for pixel intensities that are used to distinguish brighter soft-tissue structures from the darker air-containing components of the lung. The CT scanner, kilovolt potential, reconstruction algorithm, section thickness, and nodule location in the field of view have been shown to affect pixel intensity (23) and, therefore, apparent nodule diameter. Further studies are needed to establish statistical bounds on the estimation error of change-in-diameter measurements. To avoid potential sampling errors in this preliminary study, we reported the change in nodule size determined by the computer in terms of change in size category. Although assess-

ments of nodule change by the computer and radiologist correlated well with our choice of categories, a small decrease in nodule size may not have satisfied the criteria for change in category for the computer and therefore may account for some differences.

As in other preliminary studies (3,5), true- and false-positive rates reported in this study were computed for data that were used to develop the classification rules of the computer vision system. In the future, we will create a substantially larger database and separate it into training and test cases. Nodules in the training cases will be analyzed to improve the classification rules, and computer system efficacy will be assessed with test cases only and with more than one radiologist.

The computer vision system used in this study has quantitative abilities that could affect many facets of oncology care, from diagnosis of metastases to assessment of their response to chemotherapy. In the future, low-dose chest CT could be used for lung cancer screening. Use of this vision system could help ensure that nodules do not fail to be detected. In screening mammography, computer systems have been shown to improve receiver operating characteristic curves of radiologists for rating the likelihood of malignancy (24) and detecting abnormalities (25). Computer-aided diagnostic imaging systems that interact with a radiologist by means of an interface are being developed in mammography (26). Such an interface could easily be added to this computer vision system and would have many applications in thoracic radiology.

Our preliminary computer vision system demonstrates the potential for a clinically useful automated nodule detection system that quantifies nodule size and assesses for change over time. With further development, such a computer system could be applied to clinical scenarios in which objective nodule assessment is necessary.

References
1. Landis SH, Murray T, Bolden S, Wingo PA. Cancer statistics, 1999. CA Cancer J Clin 1999; 49:8–31.
2. Armato SG III, Giger ML, Moran CJ, Blackburn JT, Doi K, MacMahon H. Computerized detection of pulmonary nodules on CT scans. RadioGraphics 1999; 19:1303–1311.
3. Kanazawa K, Kawata Y, Niki N, et al. Computer-aided diagnosis for pulmonary nodules based on helical CT images. Comput Med Imaging Graph 1998; 22:157–167.
4. Henschke CI, Yankelevitz DF, Mateescu I, Brettle DW, Rainey TG, Weingard FS. Neural networks for the analysis of small pulmonary nodules. Clin Imaging 1997; 21:390–399.
5. Giger ML, Bae KT, MacMahon H. Computerized detection of pulmonary nodules in computed tomography images. Invest Radiol 1994; 29:459–465.
6. Matsumoto T, Yoshimura H, Giger ML, et al. Potential usefulness of computerized nodule detection in screening programs for lung cancer. Invest Radiol 1992; 27:471–475.
7. Xu XW, Doi K, Kobayashi T, MacMahon H, Giger ML. Development of an improved CAD scheme for automated detection of lung nodules in digital chest images. Med Phys 1997; 24:1395–1403.
8. MacMahon H, Engelmann R, Behlen FM, et al. Computer-aided diagnosis of pulmonary nodules: results of a large-scale observer test. Radiology 1999; 213:723–726.
9. Ashizawa K, MacMahon H, Ishida T, et al. Effect of an artificial neural network on radiologists' performance in the differential diagnosis of interstitial lung disease with chest radiographs. AJR Am J Roentgenol 1999; 172:1311–1315.
10. Yankelevitz DF, Gupta R, Zhao B, Henschke CI. Small pulmonary nodules: evaluation with repeat CT—preliminary experience. Radiology 1999; 212:561–566.
11. Henschke CI, McCauley DI, Yankelevitz DF, et al. Early lung cancer action project: overall design and findings from baseline screening. Lancet 1999; 354:99–105.
12. Kakinuma R, Ohmatsu H, Kaneko M, et al. Detection failures in spiral CT screening for lung cancer: analysis of CT findings. Radiology 1999; 212:61–66.
13. Horn BKP. Robot vision. Cambridge, Mass: MIT Press, 1986; 69–71.
14. Wirth N. Algorithmen und datenstrukturen. Stuttgart, Germany: Teubner, 1983; 162–185.
15. Rosner B. Fundamentals of biostatistics. 3rd ed. Belmont, Calif: Duxbury, 1990; 450–455.
16. Kapouleas I, Alavi A, Alves WM, Gur RE, Weiss DW. Registration of three-dimensional MR and PET images of the human brain without markers. Radiology 1991; 181:731–739.
17. Uematsu H, Sadato N, Yonekura Y, et al. Coregistration of FDG PET and MRI of the head and neck using normal distribution of FDG. J Nucl Med 1998; 39:2121–2127.
18. Pelizzari CA, Chen GT, Spelbring DR, Weichselbaum RR, Chen CT. Accurate three-dimensional registration of CT, PET, and/or MR images of the brain. J Comput Assist Tomogr 1989; 13:20–26.
19. Turkington TG, Jaszczak RJ, Pelizzari CA, et al. Accuracy of registration of PET, SPECT and MR images of a brain phantom. J Nucl Med 1993; 34:1587–1594.
20. Robinson AH, Bird N, Screaton N, Wraight EP, Meggitt BF. Coregistration imaging of the foot: a new localisation technique. J Bone Joint Surg Br 1998; 80:777–780.
21. Yu JN, Fahey FH, Gage HD, et al. Intermodality, retrospective image registration in the thorax. J Nucl Med 1995; 36:2333–2338.
22. Naidich DP, Webb WR, Muller NL, Krinsky GA, Zerhouni EA, Siegelman SS. Focal lung disease. In: Computed tomography and magnetic resonance of the thorax. 3rd ed. Philadelphia, Pa: Lippincott-Raven, 1999; 313.
23. Zerhouni EA, Spivey JF, Morgan RH, Leo FP, Stitik FP, Siegelman SS. Factors influencing quantitative CT measurements of solitary pulmonary nodules. J Comput Assist Tomogr 1982; 6:1075–1087.
24. Chan HP, Sahiner B, Helvie MA, et al. Improvement of radiologists' characterization of mammographic masses by using computer-aided diagnosis: an ROC study. Radiology 1999; 212:817–827.
25. Chan HP, Doi K, Vyborny CJ, et al. Improvement of radiologists' detection of clustered microcalcifications on mammograms: the potential of computer-aided diagnosis. Invest Radiol 1990; 25:1102–1110.
26. Giger M, MacMahon H. Image processing and computer-aided diagnosis. Radiol Clin North Am 1996; 34:565–596.